UDC 537.533.3; 537.534.3

INFLUENCE OF THE INTERELECTRODE GAP WIDTH ON THE QUALITY OF FOCUSING OF ELECTROSTATIC MIRRORS WITH ROTATIONAL SYMMETRY

Bimurzaev S.B. [*], Sautbekova Z.S.

G. Daukeev Almaty University of Power Engineering and Telecommunication, Almaty, Kazakhstan
***Corresponding author**: bimurzaev@mail.ru*

Abstract. *The influence of the width of the interelectrode gap on the focusing quality of electrostatic mirrors with rotational symmetry, the electrodes of which are coaxial cylinders of equal diameter separated by gaps of finite width, has been studied. Formulas, convenient for the numerical calculation of the exact values of the axial potential distribution in such mirrors, are proposed. Using the obtained formulas in numerical calculations and taking into account the width of the interelectrode gap, the geometric and electrical parameters of two- and three-electrode mirrors were determined, which provide spatial focusing of beams of charged particles simultaneously with the elimination of time-of-flight chromatic aberrations and spherical and axial chromatic spatial aberrations, the most important factors in terms of influence on the resolution of time-of-flight mass spectrometers and electron microscopes. It is shown that the width of the interelectrode gap has a significant effect on the quality of focusing of electrostatic mirrors with cylindrical electrodes.*

Keywords: time-of-flight mass spectrometer, electron microscope, electrostatic mirror, space-time-of-flight focusing, spherical aberration, axial chromatic aberration.

1. Introduction

Electrostatic mirrors are the most important structural elements of modern time-of-flight reflector-type mass spectrometers [1-5] and electron microscopes [6-14], performing the roles of an ion reflector and an aberration corrector, respectively. The resolution and sensitivity of such devices largely depend on the focusing quality of such mirrors. In this regard, electrostatic mirrors formed by fields with rotational symmetry are of particular interest. Such fields, which play the role of centered electron-optical focusing systems with respect to charged particles, are capable of creating a correct electron-optical image of an object. However, the most studied and widely used designs of such mirrors for practical implementation are sets of coaxial circular cylinders. The advantage of cylindrical electrodes is the ability to shield a beam of charged particles from scattered electric fields.

In [5, 12-14], where the quality of focusing of electrostatic mirrors with cylindrical electrodes was studied, the calculation of the axial potential distribution was performed using exact formulas under the assumption that the width of the interelectrode gap is infinitely small. However, the practical use of such mirrors places high demands on the accuracy of determining the geometric and electrical parameters, taking into account the width of the interelectrode gap, which ensures the quality of focusing in devices with high

resolution. In addition, high requirements for the width of the interelectrode gap are necessary to ensure electrostatic strength at high field strengths.
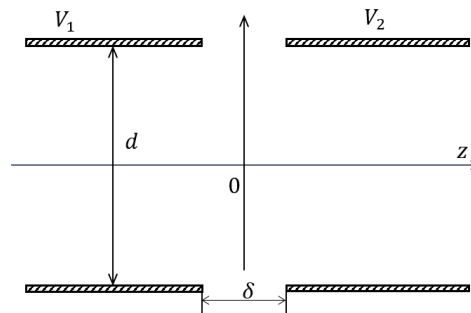
It is well known that the quality of focusing is determined by aberrations – distortions in the image of an object caused by various reasons. One of the main tasks of charged particle optics is to identify the types of aberrations inherent in a given system, and then eliminate or reduce the most important ones. In this regard, electrostatic mirrors with cylindrical electrodes have unique properties: firstly, they can provide spatial focusing of beams of charged particles simultaneously with time-of-flight energy focusing [5], i.e., eliminate time-of-flight chromatic aberrations that limit the resolution of time-of-flight mass spectrometers; secondly, they can be free from spherical and axial chromatic aberrations simultaneously [12-14] or act as a corrector for these aberrations [12], which are the main factors limiting the resolution of electron microscopes.

The aim of this work is to study the influence of the width of the interelectrode gap on the quality of focusing of two- and three-electrode mirrors with rotational symmetry, the electrodes of which are made in the form of coaxial cylinders of equal diameter, separated by gaps of finite width.

2. Two-electrode mirror with space-time focusing

2.1. Axial potential distribution of a two-electrode mirror

Figure 1 shows a schematic diagram of a two-electrode mirror, the electrodes of which are coaxial cylinders of equal diameter d separated by a gap of finite width.

V_1, V_2 are potentials on the electrodes; d is the cylinder diameter; δ is the gap width between electrodes

Fig.1. Two-electrode electrostatic mirror.

The potential distribution along the optical axis z of such a mirror can be written in the form

$$\Phi(z) = \frac{1}{2}(V_1 + V_2) + (V_2 - V_1)U(z). \tag{1}$$

Here V_1 and V_2 are potentials at the mirror electrodes, and $U(z)$ is a function described by the exact expression [15]:

$$U(z) = \frac{1}{\pi}\int_0^\infty \frac{\sin(kz)}{k}\frac{\sin(k\delta/R)}{k\delta/R}\frac{dk}{I_0(k)}, \tag{2}$$

where $I_0(k)$ is a modified Bessel function of the first kind of zero order, and R is the radius of the cylindrical electrode. To avoid the difficulties that arise when calculating integral (2) due to its weak convergence, we transformed it into a form convenient for calculations.

To simplify the notation, we will further use $R = 1$, i.e. all linear dimensions will be measured in cylinder radii. Then

$$U(z) = \frac{1}{\pi}\int_0^\infty \frac{\sin(kz)}{k}\frac{\sin(k\delta)}{k\delta}\frac{dk}{I_0(k)}. \tag{3}$$

Let us rewrite (3), writing out the product of sines:

$$U(z) = \frac{1}{2\delta}(U_1 + U_2), \tag{4}$$

where

$$U_1 = \frac{1}{\pi}\int_0^\infty \frac{\cos k(z-\delta)}{k^2}\frac{dk}{I_0(k)},$$ (5)

$$U_2 = -\frac{1}{\pi}\int_0^\infty \frac{\cos k(z+\delta)}{k^2}\frac{dk}{I_0(k)}.$$ (6)

Taking into account the parity of the integrand, and also having written the cosine, we rewrite (5) in the form

$$U_1(z) = \frac{1}{4\pi}\left[\int_{-\infty}^\infty \frac{\exp[ik(z-\delta)]}{k^2}\frac{dk}{I_0(k)} + \int_{-\infty}^\infty \frac{\exp[-ik(z-\delta)]}{k^2}\frac{dk}{I_0(k)}\right].$$ (7)

It is convenient to calculate integral (7) can using contour integrals:

$$U_1(z) = \frac{1}{4\pi}\int_{\Gamma+} \frac{\exp[ik(z-\delta)]}{k^2}\frac{dk}{I_0(k)} + \frac{1}{4\pi}\int_{\Gamma-} \frac{\exp[-ik(z-\delta)]}{k^2}\frac{dk}{I_0(k)},$$ (8)

where Γ_+ is the contour of integration along the real axis, which goes around the origin of the coordinate system from below as a narrow loop and closes it in the upper half-plane of the complex variable k by a semicircle of an infinite radius, Γ_- is a contour that consists of the real axis and closes, accordingly, in the lower half-plane (Figure 2).
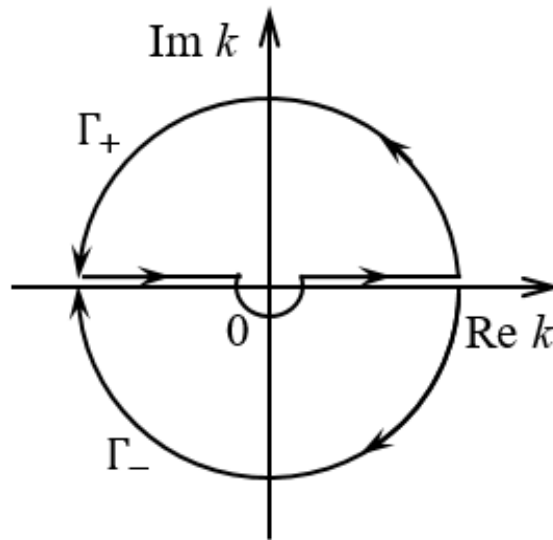

Fig.2. Integration contours on the complex plane.

Note that the contours of integration Γ_+ and Γ_-, with the exception of the vicinity of the point $k=0$, are located mirror symmetrically to each other, where the contour Γ_+ contains a second-order pole inside itself.

As the integrand is meromorphic inside the contour, the integral is equal to the sum of the residues at the poles $k=i\alpha_s$, where α_s $(s=\pm1,\pm2,...)$ are the zeros (roots) of the zero-order modified Bessel function.

Taking into account the residue at the point $k=0$, which is a simple pole of the second order

$$\operatorname{Re} s\left(\frac{\exp(ik|z-\delta|)}{I_0(k)}, k=0\right) = i|z-\delta|,$$ (9)

we can calculate the integral:

$$\frac{1}{4\pi}\int_{\Gamma+} \frac{\exp[ik(z-\delta)]}{k^2 I_0(k)}dk = -\frac{1}{2}\left[|z-\delta| + \frac{1}{2}\sum_{s=1}^\infty \frac{B_s}{\alpha_s}\exp(-\alpha_s|z-\delta|)\right].$$ (10)

Here

$$B_s = \prod_{s \neq m=1}^{\infty} \left(1 - \alpha_s^2 / \alpha_m^2\right)^{-1} \tag{11}$$

are the coefficients of the series, which follow from the representation of the modified Bessel function of zero order in the form of an infinite product:

$$I_0^*(ia_s) = \lim_{k \to i\alpha_s} \frac{I_0(k)}{k - i\alpha_s} = \frac{2i}{a_s B_s} = -I_0^*(-ia_s). \tag{12}$$

Similarly to (10), we calculate the integral:

$$\frac{1}{4\pi} \int_{\Gamma_-} \frac{\exp\left[-ik(z-\delta)\right]}{k^2} \frac{dk}{I_0(k)} = -\frac{1}{4} \sum_{s=1}^{\infty} \frac{B_s}{\alpha_s} \exp\left(-\alpha_s |z-\delta|\right). \tag{13}$$

Then, taking into account (9) - (12), expression (6) takes the form:

$$U_1 = \int_0^{\infty} \frac{\cos k(z-\delta)}{k^2 I_0(k)} dk = -\frac{1}{2}\pi \left[|z-\delta| + \sum_{s=1}^{\infty} \frac{B_s}{\alpha_s} \exp\left(-\alpha_s |z-\delta|\right) \right], \tag{14}$$

which is also valid for the case $z - \delta < 0$.

Substituting $z - \delta \to z + \delta$ we can write (6) as

$$U_2 = -\int_0^{\infty} \frac{\cos k(z+\delta)}{k^2 I_0(k)} dk = \frac{1}{2}\pi \left[|z+\delta| + \sum_{s=1}^{\infty} \frac{B_s}{\alpha_s} \exp\left(-\alpha_s |z+\delta|\right) \right]. \tag{15}$$

Taking into account (3) and (13) - (14), we finally obtain integral (3) in the form of an exponentially convergent infinite series:

$$U(z) = -\frac{1}{4\delta} \left\{ \left(|z-\delta| - |z+\delta|\right) + \sum_{s=1}^{\infty} \frac{B_s}{\alpha_s} \left[\exp\left(-\alpha_s |z-\delta|\right) - \exp\left(-\alpha_s |z+\delta|\right) \right] \right\}. \tag{16}$$

Hence, expression (3) can be written as:

$$U(z) = \frac{1}{2} \left\{ \begin{pmatrix} 1 \\ z/\delta \\ -1 \end{pmatrix} - \sum_{s=1}^{\infty} \frac{B_s}{\delta \alpha_s} \begin{bmatrix} \exp(-\alpha_s z) Sh(\alpha_s \delta), & z > \delta \\ \exp(-\alpha_s \delta) Sh(\alpha_s z), & |z| < \delta \\ -\exp(\alpha_s z) Sh(\alpha_s \delta), & z < -\delta \end{bmatrix} \right\}, \tag{17}$$

or

$$U(z) = \frac{1}{2} \left\{ \begin{array}{ll} sign(z) \left[1 - \sum_{s=1}^{\infty} \frac{B_s}{\alpha_s \delta} \exp\left(-\alpha_s |z|\right) Sh(\alpha_s \delta) \right], & |z| \geq \delta, \\[2mm] z/\delta - \sum_{s=1}^{\infty} \frac{B_s}{\alpha_s \delta} \exp\left(-\alpha_s \delta\right) Sh(\alpha_s z), & |z| < \delta, \end{array} \right\}. \tag{18}$$

For $\delta \to 0$ formula (18) transforms into a well-known expression [16]:

$$U(z) = \frac{1}{2} sign(z) \left[1 - \sum_{s=1}^{\infty} B_s \exp\left(-\alpha_s |z|\right) \right], \tag{19}$$

obtained in the other way from the exact expression [17]

$$U(z) = \frac{1}{\pi} \int_0^{\infty} \frac{\sin(kz)}{k} \frac{dk}{I_0(k)}, \tag{20}$$

also following from (3).

2.2. Space-time focusing conditions

The time-of-flight characteristics of the mirror, precise to the third smallest value inclusive, are completely determined by specifying four quantities that depend only on the axial distribution of the mirror potential [18]: $z = z_T^{(0)}$ – position of the effective plane of rotation of the central (with zero energy spread) particle in the mirror; $z = z_T^{(k)}$ $(k = 1, 2, 3)$ – positions of the nodal planes of time-of-flight focusing of the k - order.

Here and below, under the condition of time-of-flight focusing of the k-th order it is assumed that the time of flight of particles does not depend on the spread of their initial energies, i.e., the coefficient of time-of-flight chromatic aberration of the k-th order is equal to zero.

The condition of time-of-flight focusing is determined by the equation [18]:

$$z_1 + z_2 = z_T^{(k)} \qquad (k = 1, 2, 3),$$ (21)

which means that time-of-flight focusing of the k-th order is achieved if the planes $z = z_1$ (object plane) and $z = z_2$ (time-of-flight image plane) are located symmetrically with respect to the plane $z = z_T^{(k)}$ $(k = 1, 2, 3)$.

The effective drift distance, which characterizes the time-of-flight mass dispersion of the mirror, is determined by the equality [18]:

$$L = z_T^{(0)} - z_T^{(1)},$$ (22)

where $z = z_T^{(1)}$ is the position of the main plane of time-of-flight focusing of the mirror [5].

When the condition

$$z_T = z_T^{(1)} = z_T^{(2)} = z_T^{(3)}$$ (23)

is satisfied, in the plane $z = z_T$, time-of-flight focusing up to the third order inclusive can be achieved.

The condition for spatial focusing simultaneously with time-of-flight focusing, i.e., the condition for space-time-of-flight focusing is determined by equality [18]:

$$z_{1,2} = z_T \pm \sqrt{(z_T - z_C)(z - z_V)},$$ (24)

where $z = z_C$ and $z = z_V$ are the positions of the center of curvature and the vertex of the mirror, respectively, also depending only on the axial distribution of the mirror potential [21] and representing the spatial cardinal elements of the mirror.

When $z_C = z_T$ or $z_V = z_T$ equality (4) takes the form:

$$z_1 = z_2 = z_T.$$ (25)

Thus, there are two types of electrostatic mirrors in which the space-time focusing condition is satisfied. However, mirrors corresponding to the type $z_C = z_T$ have higher aperture compared to the systems corresponding to the type $z_V = z_T$ [18].

2.3. Calculation of a two-electrode mirror

The calculation of an electrostatic mirror usually starts with determining the value of the blocking potential –the potential on the reflecting electrode. In a two-electrode mirror, the blocking potential is the potential at the second electrode V_2. Its value is determined from equality (1) if the condition $\Phi(z_u) = 0$ is satisfied, where $z = z_u$ is the position of the plane of rotation of the central particle.

The calculation of a two-electrode mirror is performed as follows. For the given values of the width δ of the interelectrode gap and potentials V_1 and V_2 on the mirror electrodes, which determine the axial distribution of the potential $\Phi(z)$, the position of the main plane of time-of-flight focusing $z = z_T^{(1)}$ [5] and the effective drift distance (22) of the mirror are determined when the space-time-of-flight focusing condition (24) is satisfied in the mode $z_C = z_T$. Here and below, in order to maintain the possibility of shielding the beam from scattered electric fields, the width of the interelectrode gap is limited to the value $\delta / d <= 0.2$.

The results of calculating the time-of-flight characteristics of a two-electrode mirror depending on the width δ of the interelectrode gap are presented in Table 1. Here and below, the values of electrical parameters are given in the units of the first electrode potential V_1, and the values of geometric parameters are given in the units of the cylinder diameter d. It is accepted that a beam of charged particles falls on the mirror from the side of the field-free space having the potential V_1, and after reflection returns to the same space. In this case, the positive direction of the axis z coincides with the direction of movement of the particles falling on the mirror, and the origin of coordinates is placed in the middle of the gap (Figure 1).

As it follows from the calculated data, the relative change in the values of the blocking potential and time-of-flight characteristics compared to their values at $\delta = 0$ does not exceed one percent at the gap width

$\delta/d \leq 0.1$, whereas at the gap width $\delta/d = 0.2$ such a change is about three percent. Note that for $\delta = 0$, the results of these calculations completely coincide with the results of [5].

Table 1. Time-of-flight characteristics of a two-electrode mirror.

δ/d	$-V_2/V_1$	$-z_T/d$	L/d
0	0.345	3.30	4.17
0.05	0.345	3.30	4.17
0.1	0.344	3.32	4.20
0.15	0.342	3.35	4.24
0.2	0.340	3.40	4.29

3. Three-electrode mirror with space-time focusing

3.1. Axial potential distribution of a three-electrode mirror

Figure 3 shows a scheme of a three-electrode mirror consisting of coaxial cylinders of equal diameter.
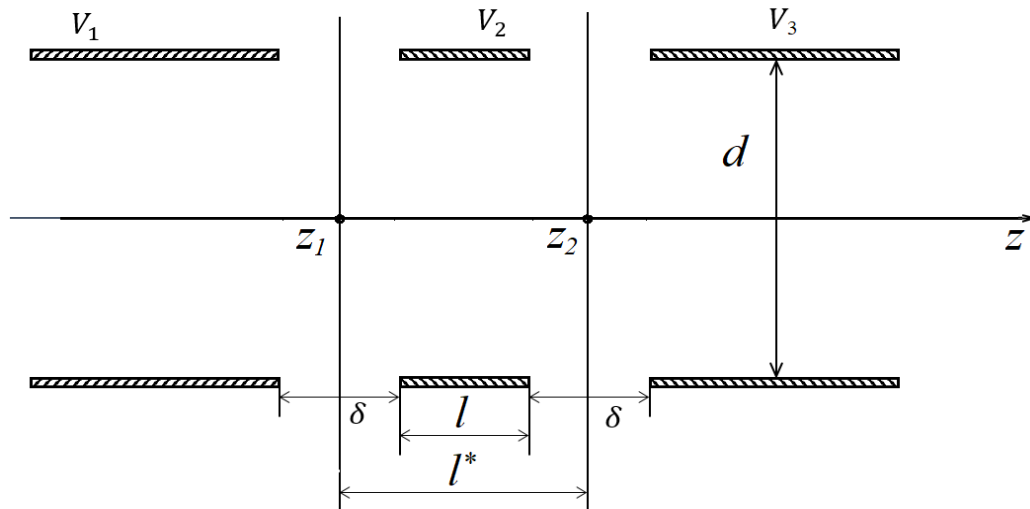

Fig.3. Three-electrode axisymmetric mirror:
V_1, V_2, V_3 are potentials on the electrodes; δ is the width of the gaps between the electrodes; z_1, z_2 are coordinates of the middle of the gaps; d is the cylinder diameter.

Using the solution to the Dirichlet problem for two cylinders of equal diameter and the superposition principle, we can write an exact formula for the axial potential distribution of a three-electrode mirror in the form:

$$\Phi(z) = \frac{1}{2}(V_1 + V_3) + \sum_{1=1}^{2}(V_{i+1} - V_i)U(z - z_i). \tag{26}$$

Here

$$U(z - z_i) = \frac{1}{2}\begin{cases} sign(z - z_i)\left[1 - \sum_{s=1}^{\infty}\dfrac{B_s}{\alpha_s\delta}\exp(-\alpha_s|z - z_i|)Sh(\alpha_s\delta), & |z - z_i| \geq \delta\right], \\ (z - z_i)/\delta - \sum_{s=1}^{\infty}\dfrac{B_s}{\alpha_s\delta}\exp(-\alpha_s\delta)Sh\left[\alpha_s(z - z_i)\right], & |z - z_i| < \delta, \end{cases} \tag{27}$$

where z_i $(i = 1, 2)$ is z coordinate of the middle of the i-th gap.

For $\delta \to 0$ formula (27) takes the well-known form [16]:

$$U\left(z-z_i\right) = \frac{1}{2} sign(z-z_i)\left[1 - \sum_{s=1}^{\infty} B_s \exp\left(-\alpha_s \left|z-z_i\right|\right)\right].$$ (28)

3.2. Calculation of a three-electrode mirror

In a three-electrode mirror, compared to a two-electrode mirror, two additional parameters appear in the form of the length of the second (middle) electrode and the potential on it, which affect the distribution of the mirror potential. The introduction of a middle electrode allows, at a given potential ratio on the outer electrodes, to control the field distribution and thereby influence the quality of space-time focusing.

In a three-electrode mirror, the blocking potential is the potential on the third electrode V_3, the value of which is determined from equality (26) when the condition $\Phi\left(z_u\right) = 0$ is satisfied.

The calculation of the three-electrode mirror is carried out as follows. For a given value of the gap width δ between the electrodes, the values of the control potential V_2 (potential on the second electrode), the blocking potential V_3 and the effective length of the second electrode (the distance between the middles of the first and second gaps) $l^* = l + \delta$, where l is the length of the second electrode, are determined. These parameters ensure fulfillment of the conditions for time-of-flight focusing of ions in energy up to the third order inclusive (3) simultaneously with spatial focusing (4) in the mode $z_C = z_T$.

The results of calculation of a three-electrode mirror with high-quality space-time focusing are presented in Table 2. In this case, the origin of coordinates is in the middle of the gap between the first and second electrodes of the mirror. As it follows from the calculated data, the relative change in the values of electrical parameters and time-of-flight characteristics compared to their values for $\delta = 0$ is of the same order of magnitude as in a two-electrode mirror.

Table 2. Time-of-flight characteristics of a three-electrode mirror

δ/d	l^*/d	V_2/V_1	$-V_3/V_1$	$-z_T/d$	L/d
0	0.666	0.0432	0.342	5.56	7.22
0.05	0.668	0.0433	0.342	5.57	7.24
0.1	0.672	0.0439	0.342	5.60	7.28
0.15	0.680	0.0449	0.343	5.65	7.34
0.2	0.690	0.0461	0.343	5.72	7.43

4. Three-electrode mirror free of spherical and axial chromatic aberration

The calculation of the spherical and axial chromatic aberrations of the three-electrode mirror was carried out according to the formulas [19, 20]. In this case, a mirror is calculated with a second electrode length equal to $l/d = 0.6$, and the object plane of the mirror is combined with its focal plane, as in [13].

The mirror was calculated using the same method as in the previous section. For a given value of the width δ of the interelectrode gap, the values of the control potential V_2 (potential on the second electrode) and the blocking potential V_3, ensuring fulfillment of the conditions for simultaneous elimination of the third-order spherical aberration and the second-order axial chromatic aberration, are determined.

The calculation results are presented in Table 3, which presents the dependences of the relative changes in the values of the cardinal elements of the mirror (focus coordinate z_F and focal length f) and the potential ratios on its electrodes (V_2 and V_3) on the width of the interelectrode gap. In this case, the calculation results are presented for the case when the object plane of the mirror is combined with its focal plane, as it was done earlier for an infinitesimal width of the interelectrode gap $\left(\delta = 0\right)$ [13].

It should be noted that the width of the interelectrode gap has a significant (an order of magnitude or more) influence on the values of the electrical parameters and cardinal elements of the mirror, which is simultaneously free of spherical and axial chromatic aberrations.

For $\delta = 0$ the results of these calculations completely coincide with the results of [13].

Table 3. Three-electrode mirror free of spherical and axial chromatic aberrations.

δ/d	V_2/V_1	$-V_3/V_1$	$-z_F/d$	f/d
0	0.0255	0.292	0.948	1.85
0.05	0.0258	0.294	0.982	1.88
0.1	0.0266	0.303	1.10	1.99
0.15	0.0285	0.318	1.38	2.24
0.2	0.0328	0.347	2.14	2.96

5. Conclusion

The exact formula for the axial distribution of the potential of an electrostatic system consisting of coaxial cylinders of equal diameter separated by gaps of finite width is reduced to a form convenient for numerical calculations. Using the obtained formula in numerical calculations, the influence of the width of the interelectrode gap on the quality of focusing of two- and three-electrode electrostatic mirrors with rotational symmetry, the electrodes of which are coaxial cylinders of equal diameter separated by gaps of finite width, is studied. As the results of these studies have shown, taking into account the width of the interelectrode gap allows not only to obtain more accurate values of geometric and electrical parameters that provide the conditions for high-quality space-time focusing in such mirrors, but also to provide them additional functionality, in particular, with increasing width of the interelectrode gap the effective distance of the mirror increases, which, accordingly, leads to an increase in the resolution of the time-of-flight mass spectrometer.

It should be noted that the width of the interelectrode gap has a significant impact on the values of the electrical parameters and cardinal elements of the mirror, which is free of spherical and axial chromatic aberrations simultaneously. This confirms the particular relevance of such studies from the point of view of the accuracy of calculations in the field of high-voltage electron microscopy, where the interelectrode gaps must have a width sufficient to ensure the electrostatic strength of the mirror electrodes of a real design.

The results and formulas obtained in this work can be used in the development of new designs of time-of-flight mass spectrometers and electron microscopes with high resolution and sensitivity.

References

1 Mamyrin B.A. (2001) Time-of-flight mass spectrometry (concepts, achievements, and prospects). *Int. J. Mass Spectrometry*, 206 (3), 251-266. DOI: 10.1016/S1387-3806(00)00392-4.

2 Wollnik H., Casares A. (2003) An energy-isochronous multi-pass time-of-flight mass spectrometer consisting of two coaxial electrostatic mirrors. *Int. J. Mass Spectrometry*, 227 (2), 217-222. DOI: 10.1016/S1387-3806(03)00127-1.

3 Yavor M., Verentchikov A., Hasin Y., Kozlov B., Gavrik M., Trufanov A. (2008) Planar multi-reflecting time-of-flight mass analyzer with a jig-saw ion path. *Physics Procedia,* 1 (1), 391-400. DOI: 10.1016/j.phpro.2008.07.120.

4 Spivak-Lavrov I., Baisanov O., Yakushev E., Nazarenko L. (2019) TOF mass spectrometers based on a wedge-shaped electrostatic mirror with a two-dimensional field. *Rapid Communications in Mass Spectrometry,* 34(4). DOI:10.1002/rcm.8590.

5 Bimurzaev S.B., Aldiyarov N. U., Sautbekova Z.S. (2020) High Dispersive Electrostatic Mirrors of Rotational Symmetry with the Third Order Time-of-Flight Focusing by Energy. *Technical Physics*, 65, 1150–1155. DOI:10.1134/S1063784220070051.

6 Rempfer G.F. (1990) A theoretical study of the hyperbolic electron mirror as a correcting element for spherical and chromatic aberration in electron optics. *J.Appl. Phys*., 67 (10), 6027-6040. DOI: 10.1063/1.345212.

7 Preikszas D., Rose H. (1997) Correction properties of electron mirrors. *Microscopy*, 46 (1), 1-9. DOI:10.1093/oxfordjournals.jmicro.a023484.

8 Hartel P., Preikszas D., Spehr R., Muller H., Rose H. (2002) Mirror corrector for low-voltage electron microscopes. *Adv. Imaging & Electron Phys*., 120, 41-133. DOI: 10.1016/S1076-5670(02)80034-9.

9 Hawkes P.W. (2009) Aberration correction past and present. *Phil. Trans. R. Soc.* DOI: 10.1098/rsta.2009.0004.

10 Tromp R.M., Hannon J.B., Wanb W., Berghaus A., Schaff O. (2010) A new aberration-corrected, energy-filtered LEEM/PEEM instrument. I. Principles and design. *Ultramicroscopy,* 110 (7), 852-861. DOI:10.1016/j.ultramic.2010.03.005.

11 Tromp R.M., Hannon J.B., Wanb W., Berghaus A., Schaff O. (2013) A new aberration-corrected, energy-filtered LEEM/PEEM instrument. II. Operation and results. *Ultramicroscopy*, 127, 25-39. DOI:10.1016/j.ultramic.2012.07.016.

12 Bimurzaev S.B., Aldiyarov N.U., Yakushev E.M. (2017) The objective lens of the electron microscope with correction of spherical and axial chromatic aberrations, *Microscopy,* 66 (5), 356-365. DOI: 10.1093/jmicro/dfx023.

13 Bimurzaev S.B., Serikbaeva G.S., Yakushev E.M. (2003) Electrostatic Mirror Objective with Eliminated Spherical and Axial Chromatic Aberrations. *Microscopy*, 52 (4), 365-368. DOI: 10.1093/jmicro/52.4.365.

14 Bimurzaev S.B., Yakushev E.M. (2022) Relativistic Theory of Aberrations of Electrostatic Electron-Optical Systems. *Nucl. Instr. Meth. Phys. Res. A*., 1022, 1-10. DOI: 10.1016/j.nima.2021.165956.

15 Zhu X., Munro E. (1995) Second-Order Finite Element Method and its Practical Application in Charged Particle Optics. *Journal of Microscopy*, 179(2), 172 – 180. DOI: 10.1111/j.1365-2818.1995.tb03629.x.

16 Bobykin B.V., Nevinnyi Yu.A., Yakushev E.M. (1975). Electron-optical lens as a preliminary accelerator of slow electrons in beta-spectrometry. *Zhurnal Tekhnicheskoi Fiziki*, 45, 2368–2372.

17 Gray F. Electrostatic electron-optics (1939) *Bell. Syst. Techn. Journ*., 18(1), 1-31. DOI: 10.1002/j.1538-7305.1939.tb00805.x.

18 Bimurzaev S.B., Bimurzaeva R.S., Sarkeev B.T. (1991) Spatial and time-of-flight focusing in an electrostatic lens-mirror system with two planes of symmetry. *Radiotekhnika I Elektronika*, 36, 2186–2195.

19 Yakushev E.M., Sekunova L.M. (1986) Theory of electron mirrors and cathode lenses. *Advances in Electronics and Electron Physics,* 68, 337–416. DOI: 10.1016/S0065-2539(08)60856-2.

20 Yakushev, E. M. (2013). Theory and computation of electron mirrors: The central particle method. *Advances in Imaging and Electron Physics*, *178*, 147–247. Elsevier. DOI: 10.1016/B978-0-12-407701-0.00003-0.

_____

AUTHORS' INFORMATION

Bimurzaev, Seitkerim - Professor, Doctor of Physics and Mathematics, Chief Researcher, G. Daukeev Almaty University of Power Engineering and Telecommunication, Almaty, Kazakhstan; Scopus Author ID: 6603367014, Web of Science Researcher ID: Q-9680-2016, ORCID: 0000-0001-7778-1536; bimurzaev@mail.ru

Sautbekova, Zerde – PhD, Researcher, G. Daukeev Almaty University of Power Engineering and Telecommunication, Almaty, Kazakhstan; Scopus Author ID: 55946640100, ORCID ID: 0000-0001-9198-4524, zerdesautbekova@yandex.ru

.